

The Effect Of High Chloride Concentration On Stress Corrosion Cracking Behaviour Of Copper

NWMO TR-2008-12

December 2008

B.M. Ikeda¹

C.D. Litke²

1. University of Ontario Institute of Technology
2. Atomic Energy of Canada Limited

nwmo

NUCLEAR WASTE
MANAGEMENT
ORGANIZATION

SOCIÉTÉ DE GESTION
DES DÉCHETS
NUCLÉAIRES



Nuclear Waste Management Organization
22 St. Clair Avenue East, 6th Floor
Toronto, Ontario
M4T 2S3
Canada

Tel: 416-934-9814
Web: www.nwmo.ca

**The Effect of High Chloride Concentration on Stress Corrosion
Cracking Behaviour of Copper**

NWMO TR-2008-12

December 2008

B.M. Ikeda¹

C.D. Litke²

1. University of Ontario Institute of Technology

2. Atomic Energy of Canada Limited

Disclaimer:

This report does not necessarily reflect the views or position of the Nuclear Waste Management Organization, its directors, officers, employees and agents (the "NWMO") and unless otherwise specifically stated, is made available to the public by the NWMO for information only. The contents of this report reflect the views of the author(s) who are solely responsible for the text and its conclusions as well as the accuracy of any data used in its creation. The NWMO does not make any warranty, express or implied, or assume any legal liability or responsibility for the accuracy, completeness, or usefulness of any information disclosed, or represent that the use of any information would not infringe privately owned rights. Any reference to a specific commercial product, process or service by trade name, trademark, manufacturer, or otherwise, does not constitute or imply its endorsement, recommendation, or preference by NWMO.

ABSTRACT

Title: The Effect of High Chloride Concentration on Stress Corrosion Cracking Behaviour of Copper
Report No.: NWMO TR-2008-12
Author(s): B.M. Ikeda¹ and C.D. Litke²
Company: 1. University of Ontario Institute of Technology
2. Atomic Energy of Canada Limited
Date: December 2008

Abstract

In this study, the effect of high concentrations of chloride on the stress corrosion cracking (SCC) behaviour of oxygen free phosphorous doped (OFP) copper was investigated in nitrite, ammonia, and acetate environments at room temperature. All experiments in the study were constant extension rate tests using a compact tension specimen under a galvanically applied current of $1 \mu\text{A}\cdot\text{cm}^{-2}$. The corrosion potential was measured during each experiment. The experimental findings are summarized as follow:

- In a $0.1 \text{ mol}\cdot\text{L}^{-1}$ nitrite solution, copper could be subjected to extensive SCC in the presence of $\leq 0.01 \text{ mol}\cdot\text{L}^{-1}$ (i.e., $\sim 0.6 \text{ g}\cdot\text{L}^{-1}$) NaCl. However, the addition of $0.1 \text{ mol}\cdot\text{L}^{-1}$ ($\sim 6 \text{ g}\cdot\text{L}^{-1}$) and $5.5 \text{ mol}\cdot\text{L}^{-1}$ (i.e., $\sim 320 \text{ g}\cdot\text{L}^{-1}$) NaCl would suppress SCC.
- In a $1 \text{ mol}\cdot\text{L}^{-1}$ ammonia solution, copper could be subjected to extensive SCC in the absence of NaCl and in the presence of $0.5 \text{ mol}\cdot\text{L}^{-1}$ ($\sim 30 \text{ g}\cdot\text{L}^{-1}$) NaCl. However, the addition of $\sim 5.5 \text{ mol}\cdot\text{L}^{-1}$ ($\sim 320 \text{ g}\cdot\text{L}^{-1}$) NaCl would suppress SCC.
- In a $0.1 \text{ mol}\cdot\text{L}^{-1}$ acetate solution, copper could be susceptible to SCC in the presence of $\leq 0.01 \text{ mol}\cdot\text{L}^{-1}$ NaCl. However, the extent of SCC would be limited. The addition of higher concentrations of NaCl (0.1 and $\sim 5.5 \text{ mol}\cdot\text{L}^{-1}$, i.e., $6 \text{ g}\cdot\text{L}^{-1}$ and $320 \text{ g}\cdot\text{L}^{-1}$) suppressed SCC and only ductile tearing was observed for the copper specimens.

The present study appears to indicate a high concentration of $\sim 5.5 \text{ mol}\cdot\text{L}^{-1}$ ($\sim 320 \text{ g}\cdot\text{L}^{-1}$) NaCl would suppress SCC in nitrite, ammonia, and acetate solutions. The high NaCl concentration would suppress SCC by promoting uniform corrosion and disrupting oxide film formation on the crack surface. The stress corrosion factor (SCCF1), surface crack extension rate (SCER), and visual examination of the copper specimens suggested ductile behaviour in high chloride concentrations.

TABLE OF CONTENTS

	<u>Page</u>
ABSTRACT	v
1. INTRODUCTION	1
2. EXPERIMENTAL	2
2.1 MATERIALS AND SPECIMENS	2
2.2 EQUIPMENT	2
2.2.1 Constant Extension Rate Tests	2
2.3 SOLUTIONS	3
2.4 POST-TEST ANALYSES	3
3. RESULTS AND DISCUSSION	4
3.1 EFFECT OF HIGH CHLORIDE CONCENTRATION IN 0.1 mol·L⁻¹ NITRITE SOLUTION	4
3.2 EFFECT OF HIGH CHLORIDE CONCENTRATION IN 1.0 mol·L⁻¹ AMMONIA SOLUTION	6
3.2.1 Effect of High Chloride Concentration in Ammonia Solutions (No Added Copper)	6
3.2.2 Effect of High Chloride Concentration in Ammonia Solutions with Added Copper	6
3.3 EFFECT OF HIGH CHLORIDE CONCENTRATION IN 0.1 mol·L⁻¹ ACETATE SOLUTION	7
4. CONCLUSIONS	8
ACKNOWLEDGEMENTS	9
REFERENCES	10

LIST OF TABLES

	<u>Page</u>
Table 1: Summary of Chloride Experiments Performed* at Room Temperature.....	12
Table 2: Summary of Comparative Experimental Results in All Environments	13
Table 3: Summary of Experiments as a Function of Chloride Concentration in 0.1 mol·L ⁻¹ Nitrite Solutions	14
Table 4: Summary of Experiments as a Function of Chloride Concentration in 1 mol·L ⁻¹ Ammonia Solutions.....	14
Table 5: Summary of Experiments as a Function of Chloride Concentration in 0.1 mol·L ⁻¹ Acetate Solutions.....	15

LIST OF FIGURES

	<u>Page</u>
Figure 1: Schematic of SKB4 Plate Material Showing the Location of Specimen Cuts.	16
Figure 2: Compilation of SCC behaviour for OFP Cu in Chloride-containing deaerated 0.1 mol·L ⁻¹ Nitrite solution.....	17
Figure 3: Compilation of SCC behaviour for OFP Cu in Chloride-containing aerated 1 mol·L ⁻¹ Ammonia solution without added copper.....	19
Figure 4: Compilation of SCC behaviour for OFP Cu in Chloride-containing aerated 1 mol·L ⁻¹ Ammonia solution with 4 mmol·L ⁻¹ added copper.	21
Figure 5: Compilation of SCC behaviour for OFP Cu in Chloride-containing deaerated 0.1 mol·L ⁻¹ Acetate solution.	23

1. INTRODUCTION

Oxygen free phosphorous-doped (OFP) copper has been selected as the corrosion-barrier material for used-fuel containers that would be used to contain and isolate used fuel in a deep geological repository (DGR) (Maak 1999). Predicting the lifetime performance of container materials under various environments and for various degradation mechanisms is an important component of assessing the performance of the repository system.

Stress corrosion cracking (SCC) is a well-known phenomenon for copper and copper alloys. Three conjoint factors are required for SCC: a susceptible material, an appropriate environment, and sufficient tensile stress. In previous Canadian studies, experiments were carried out to investigate the SCC behaviour in nitrite/chloride, ammonia/chloride (Ikeda and Litke 2000, 2004), and acetate environments (Litke and Ikeda 2006). Copper has been shown to be susceptible to SCC in nitrite (King et al. 1999a), ammonia (Ikeda and Litke 2004), and acetate environments (Cassange et al. 1990, Honda et al. 1999).

Previous studies indicated that SCC susceptibility and crack growth are closely related to the nitrite and ammonia concentrations, corrosion potential values, and mechanical loading conditions (Ikeda and Litke 2000, 2004). In addition, the SCC susceptibility appears to be suppressed by the presence of chloride. The test results also indicate that a $\text{Cu}_2\text{O}/\text{CuO}$ surface oxide film must be present for SCC to occur. The formation of the surface oxide film depends on the potential of the system. A stress corrosion cracking model has been developed for predicting the occurrence of SCC on copper containers in a DGR (King and Kolar 2005). The model accounts for SCC of copper containers due to the presence of SCC agents and a corrosion potential that promotes the formation of the surface oxide film.

The available experimental data that can be used for predicting SCC of copper containers in acetate environments under repository conditions are limited. Both SKB and POSIVA have recognized the need to develop more SCC experimental data to define boundary conditions for SCC of copper in acetate environments (King et al. 2001, 2002).

Two environmental conditions that are expected to mitigate against SCC of the container are the lack of oxidant and the presence of chloride ion in a DGR (King et al. 1999a). As with other corrosion processes, the lack of oxidant and the slow rate at which it will diffuse to the container surface are expected to limit the rate and extent of SCC. There is some evidence that chloride ions inhibit the SCC of brass and copper in ammonia solutions (King et al. 1999b, Ikeda and Litke 2004), and similar behaviour might be expected in other environments. The inhibitive effect of chloride may involve disruption of the oxide film, important in a number of SCC mechanisms, or the promotion of general dissolution over passive behaviour. Regardless, chloride will be present in the DGR host rock media because of the predominance of chloride-based groundwaters found in candidate crystalline or sedimentary rock formations.

The purpose of this project is to develop experimental copper stress corrosion cracking (SCC) data that can be employed together with the SCC model, to support the assumption that stress corrosion cracking will not have a significant impact on the integrity or long-term performance of a copper used-fuel container during its design lifetime in a deep geologic repository. The objectives of the SCC program within the NWMO Technical Research and Development Program are to:

- i) Improve our knowledge and understanding of the conditions which may lead to SCC of copper in a deep geologic repository for used fuel; and
- ii) Determine the boundaries for the environmental parameters affecting SCC of copper.

This report describes the results of room temperature constant-extension rate tests performed with each of the SCC agents, nitrite, ammonia and acetate, and in the presence of chloride. These tests were designed to study the effect of high chloride concentration on the SCC of OFP copper obtained from the SKB.

2. EXPERIMENTAL

2.1 MATERIALS AND SPECIMENS

Compact tension (CT) coupons were prepared from the SKB-4 OFP copper plate sections C1D and C1E, as described previously (Ikeda and Litke 2000). The pre-crack was generated using a carefully regulated fatigue crack-growth procedure with a Universal Testing machine. All specimens tested had the fatigue crack oriented in the T-S orientation (see Figure 1).

The overall shape of the CT specimens follows the specification outlined in ASTM-E 399-90 (ASTM 1994). The ratio of the specimen dimensions conform to this standard, but because of the low strength of copper, the overall dimensions do not. The standard requires physically larger specimens to be used to maintain appropriate plane-strain fracture conditions for a low strength material such as copper. Such specimens would be unreasonable for laboratory testing. The overall SCC behaviour can be compared for a consistent set of specimens although the estimated (ASTM 1994) stress intensity factor (K_Q) and crack velocity are not strictly valid for the application of plane strain fracture mechanics. The values may be used to qualitatively compare the crack growth for various environmental and loading conditions. Ductile tearing and measurement errors caused by the loss of surface planarity will contribute to the estimated values for the surface crack velocity (SCER) and K_Q for the onset of SCC reported here.

2.2 EQUIPMENT

2.2.1 Constant Extension Rate Tests

The constant extension rate test (CERT) involves a continuous loading of the specimen by increasing the distance between the loading holes at constant rate. These experiments were performed in the slow strain rigs described previously (e.g., Ikeda and Litke 2000). A registered, small-volume pressure vessel with a PTFE liner was used as the cell body. The internal arrangement of the vessel was the same as reported previously for room temperature experiments (King et al. 1999a). CONAX pressure fittings with PTFE inner-sealing ferrules were used to permit electrode connections to penetrate the pressure vessel head yet maintain both electrical isolation and the pressure boundary seal.

All experiments reported were performed in ~0.5 L of solution at room temperature (22°C) and the specimens were pulled at a constant cross-head speed of $8.5 \times 10^{-6} \text{ mm}\cdot\text{s}^{-1}$. A summary of the experimental conditions is presented in Table 1.

The experiments were performed under galvanostatic (applied current of $1 \mu\text{A}\cdot\text{cm}^{-2}$) conditions. These experiments were performed using a platinum mesh counter electrode and a Thompson ministat for applying the constant current, as described previously (e.g., King et al. 1999a). The potentials were measured against a commercially available saturated calomel electrode (SCE) and all potentials are reported against this electrode. The redox potential was not measured during the galvanostatic experiments. However, at the end of these experiments, but before opening the vessel to the atmosphere, the current was removed from the specimens and the counter electrode was allowed to re-equilibrate with the test solution. The potential of the platinum mesh was measured against the SCE and the value recorded as the final solution redox potential.

The load sustained by the CT specimen as a result of its extension was measured using a load cell attached to both the specimen and the load frame. The output from this cell was recorded and used to generate a load curve. The nominal extension was measured using a displacement gauge. The data were recorded at 60 s intervals, using an in-house data acquisition program powered by LABVIEW Version 8.0, running on a Compaq Deskpro Pentium computer with a Windows XP Professional, Version 2002 Service Pack 2, operating system.

2.3 SOLUTIONS

All four of the previously studied solution environments, (deaerated $0.1 \text{ mol}\cdot\text{L}^{-1}$ sodium nitrite pH 9, deaerated $0.1 \text{ mol}\cdot\text{L}^{-1}$ sodium acetate pH 9, and aerated $1.0 \text{ mol}\cdot\text{L}^{-1}$ ammonia pH 12 both with and without $4 \text{ mmol}\cdot\text{L}^{-1}$ copper), were saturated with sodium chloride (NaCl) (approx. $5.5 \text{ mol}\cdot\text{L}^{-1}$ or $\sim 320 \text{ g}\cdot\text{L}^{-1}$). As chloride had not been added to the previous ammonia work (Litke and Ikeda 2006), supplementary tests containing $0.5 \text{ mol}\cdot\text{L}^{-1}$ (i.e., $\sim 30 \text{ g}\cdot\text{L}^{-1}$) NaCl were also performed in the ammonia environments.

The saturated chloride solution was prepared by using an excess of sodium chloride salt and a finite volume of millipore water. The solution was stirred and allowed to equilibrate for 24 hours. The resulting solution was decanted off for use. Aliquots of the saturated NaCl solution were analyzed and the concentration of NaCl was found to be $\sim 5.5 \text{ mol}\cdot\text{L}^{-1}$ ($320 \text{ g}\cdot\text{L}^{-1}$). The nitrite and acetate solutions were prepared by dissolving the appropriate mass of salt in a saturated sodium chloride solution, then adjusting the pH to 9.0 using dilute NaOH. The ammonia solutions were prepared by diluting a known volume of concentrated ($7.4 \text{ mol}\cdot\text{L}^{-1}$) ammonia with the millipore purified deionised water or saturated sodium chloride solution, then measuring the resulting pH. The pH was measured using a commercial glass pH electrode. Solutions were prepared using reagent grade chemicals.

2.4 POST-TEST ANALYSES

Following the experiment, aliquots of the test solution were submitted for chemical analysis: by ion-coupled plasma spectroscopy to determine the total dissolved copper concentrations; and by ion chromatograph to determine/confirm base chloride concentration for a saturated solution.

At the end of each experiment, a visual examination of the specimen was performed and features were noted. The specimen was then digitally imaged, and the images printed and stored for future reference. The crack extension and crack-mouth opening values were measured from the overview sample image. The stress intensity factor (K_Q) at the onset of

cracking was estimated using the initial surface fatigue crack length and the 5% secant load (ASTM 1994). The ratio of the specimen opening to the crack extension has been found to be an empirical indication of SCC and this factor (SCCF1), along with the surface crack extension rate (SCER), was calculated as described previously (Ikeda and Litke 2000).

3. RESULTS AND DISCUSSION

A summary of the data for all experiments performed in this study is presented in Table 1. The surface crack extension rate and SCCF1 values are indicators of crack growth behaviour. In the experiments performed in the saturated chloride ($\sim 5.5 \text{ mol}\cdot\text{L}^{-1}$ or $\sim 320 \text{ g}\cdot\text{L}^{-1}$ NaCl) solutions, the data suggests strictly ductile behaviour. In contrast, the experiments performed in the ammonia environments with $0.5 \text{ mol}\cdot\text{L}^{-1}$ chloride (i.e., $\sim 30 \text{ g}\cdot\text{L}^{-1}$ NaCl) produced specimens with brittle-like SCC crack-growth behaviour.

Very high SCCF1 values (> 5) are clear indications of ductile behaviour, and very low values (< 2.5) are clear indications of brittle-like SCC. Intermediate values of SCCF1 indicate a mixture of brittle-like and ductile cracking behaviour. An extensive visual examination of the crack is required to determine the degree of brittle-like behaviour (Litke and Ikeda 2006).

The data for Table 2 were extracted from our current and previous studies, and represent a series of experiments for which only the chloride concentration was changed. The visual observations describing the appearance of the specimens following the tests are included in Table 2. The overall effect of chloride will be discussed in this report and further analysis of the intermediate cracking behaviour will be deferred to future reports.

3.1 EFFECT OF HIGH CHLORIDE CONCENTRATION IN $0.1 \text{ mol}\cdot\text{L}^{-1}$ NITRITE SOLUTION

The effect of chloride concentration on SCC of OFP copper in deaerated $0.1 \text{ mol}\cdot\text{L}^{-1}$ NaNO_2 at pH 9 was examined using $1 \mu\text{A}\cdot\text{cm}^{-2}$ galvanostatic current to simulate cathodic-diffusion-controlled corrosion of the specimen. The NaCl concentration was varied from 0 (no added chloride) to saturation and the results are summarized in Table 3. The load- and potential-transient plots are shown in Figure 2, with an overview image of the specimen following the completion of each nitrite experiment shown to the left of each graph.

A saturated NaCl solution was used for experiment CERT107; the measured potential was negative, the load decay was slow, the appearance of the specimen was rough, etched, and oxidized (Figure 2), and the copper concentration measured in the solution at the end of the experiment was high (Table 3). The appearance of the specimen and the negative corrosion potential are consistent with active corrosion. At $0.1 \text{ mol}\cdot\text{L}^{-1}$ NaCl concentration (CERT35), the potential was more positive than in CERT107 (Figure 2), but the specimen appearance, the slow load decay (Figure 2), the small SCER, and the large SCCF1 value (Table 3) were consistent with uniform corrosion and an absence of SCC. The specimen surface was coated with a heavy, friable coating that was easily disturbed. This layer was probably precipitated from solution, which is consistent with a low copper concentration in solution. The measured potential for both these experiments was negative, and the specimens showed only ductile tearing with no evidence for SCC. A comparison of the appearance of these specimens showed significant differences, the most notable being the presence of a film following experiment CERT35. However, each specimen suffered extensive corrosion and the rate of copper dissolution was sufficiently rapid that crack tip blunting appeared to prevent stress intensification

and crack growth. The large SCCF1 values (> 5) and small SCER values (near $2 \text{ nm}\cdot\text{s}^{-1}$) reported in Table 3 suggest ductile behaviour with no brittle-like cracking. This is consistent with the flat load curve. The slow decrease in load is consistent with a small change in load bearing area caused by plastic deformation of the specimen. In contrast, a rapid decrease in load would be consistent with a rapid loss in load bearing area caused by fast crack extension into the load bearing region of the specimen.

Specimens exposed to lower or zero chloride concentrations ($\leq 0.01 \text{ mol}\cdot\text{L}^{-1}$) were similar in appearance. Each specimen showed a mottled appearance with patches of a bluish/brown precipitate (Figure 2). A low copper concentration was measured in the solution following these experiments (Table 3). The load curve decreased rapidly during the experiment, a positive corrosion potential was observed (Figure 2), the SCCF1 factor was not large, and the SCER was $> 2 \text{ nm}\cdot\text{s}^{-1}$ (Table 3). Although an explicit correlation between the corrosion potential and chloride concentration is not apparent, a corrosion potential between 0.00 and $0.15 V_{\text{SCE}}$ appears to indicate susceptibility to SCC. Decreasing the chloride concentration appears to cause the load curve to decay more rapidly, indicating that OFP Cu is sensitive to SCC at lower chloride concentrations. A description of the effect of increasing the chloride concentration on SCC in nitrite solutions has been reported previously (King et al 1999b, Ikeda and Litke 2000).

It is well known that the presence of an oxide film on copper is a necessary condition before SCC can occur, but the characteristics of that film have not been established. The positive potential values measured for the specimens that exhibited SCC are consistent with the formation of a surface film. The appearance of the specimens also suggests the presence of a film. However, the visible appearance of a film is not sufficient to indicate SCC. The thickest oxide film was found covering the specimen from experiment CERT35, but the specimen did not crack. The potential for the specimen was negative, suggesting active corrosion. This is consistent with the process described by Bertocci et al. (1990) where the initial film growth process is a solid state reaction to form a thin, adherent Cu_2O layer. This layer is not susceptible to cracking, similar to the behaviour of the coppery-coloured specimens presented here. The second step in the Cu_2O film growth process was thought to require the generation of a porous Cu_2O solid state film with a precipitated Cu_2O layer on top (Bertocci et al. 1990). SCC was observed when the precipitated layer was not too thick (Bertocci et al 1990). Our results indicate that SCC occurs when some black tarnish is present, but SCC does not occur when a precipitated film is present.

Increasing the chloride concentration in solution appears to increase the active corrosion of OFP copper in nitrite solution. This increased rate may be assisted by the formation of copper complex ions in solution. Such a process would favour the dissolution of copper over the formation of a copper solid on the metal surface, that is, increasing the solubility of copper in solution. This is consistent with the absence of a surface film and the high solution concentration of copper observed for experiment CERT107 (saturated chloride).

The specimens exposed to a base solution of $0.1 \text{ mol}\cdot\text{L}^{-1}$ nitrite showed an increasing degree of ductile behaviour (deformation at the crack-tip) with increasing chloride concentration (Figure 2). Only ductile tearing with no SCC was observed when the concentration of chloride was greater than or equal to $0.1 \text{ mol}\cdot\text{L}^{-1}$. This is consistent with previous work where a 1:1 NO_2/Cl^- concentration ratio was found to be sufficient to inhibit SCC of OFP copper (Ikeda and Litke 2000, King et al. 1999a).

SCC was not observed on OFP copper exposed to a saturated chloride solution of $0.1 \text{ mol}\cdot\text{L}^{-1}$ nitrite. High chloride concentrations appeared to increase the corrosion of OFP copper, which

coincided with a blunting of the crack tip. The susceptibility to SCC appeared to increase with decreasing chloride concentration. The OFP Cu was also susceptible to SCC in chloride free nitrite solutions.

3.2 EFFECT OF HIGH CHLORIDE CONCENTRATION IN 1.0 mol·L⁻¹ AMMONIA SOLUTION

The SCC behaviour of OFP Cu in ammonia solutions was different than in either acetate or nitrite solutions. A definite potential transition was observed that coincided with the onset of brittle-like crack growth. Thus, an initial ductile region could be observed on the specimen before the brittle-like cracking region. Adding copper to solution improved the reproducibility of the SCC behaviour. Consequently, the absence of SCC in chloride-free solutions does not preclude the possibility of SCC after a longer exposure, but the absence of SCC in copper containing solution does provide strong evidence for the absence of SCC at any time.

Two series of SCC tests were performed, one without added copper and one with 4 mmol·L⁻¹ added copper. All tests were performed galvanostatically, at 1 $\mu\text{A}\cdot\text{cm}^{-2}$ applied current, in 1 mol·L⁻¹ ammonia at pH 12 without deaeration. The NaCl concentration varied from 0 mol·L⁻¹ to saturation (~5.5 mol·L⁻¹ or ~320 g·L⁻¹ NaCl). The results are summarized in Table 4. The solutions with no added NaCl were found to contain a trace of chloride (< 0.02 mol·L⁻¹) at the end of the experiment, which suggests a slight leakage from the reference electrode during the experiment. The load- and potential-transient plots are shown in Figures 3 and 4, with an overview image of the specimen following the completion of each ammonia experiment shown to the left of each graph.

With the addition of 0.5 mol·L⁻¹ chloride (~30 g·L⁻¹ NaCl), the potential transition for SCC occurs at a slightly more negative value (-0.420V) than without added chloride (-0.400V). This applies to both series of ammonia solutions.

3.2.1 Effect of High Chloride Concentration in Ammonia Solutions (No Added Copper)

Stress corrosion cracks were found in copper specimens tested in 1 mol·L⁻¹ ammonia solution, i.e., CERT110, CERT66, and CERT67 (Figure 3, and Table 2). The addition of 0.5 mol·L⁻¹ (~30 g·L⁻¹) NaCl was not sufficient to suppress SCC (CERT110). The load transients for these specimens were relatively flat for most of the testing period, but decayed rapidly near the end of the test (see Figure 3). This trend suggests an initial long period of ductile tearing with little SCC, and the onset of SCC close to the end of the testing period. The values for SCCF1 and SCER for these experiments (Table 4) are consistent with a mixture of both SCC and ductile cracking.

The result of CERT111 indicated that a chloride concentration of ~5.5 mol·L⁻¹ would suppress SCC. The load curve for experiment CERT111 was flat throughout (Figure 3), indicating only ductile tearing of the specimen.

3.2.2 Effect of High Chloride Concentration in Ammonia Solutions with Added Copper

The addition of 4 mmol·L⁻¹ of copper to the aerated 1 mol·L⁻¹ ammonia solution was found to improve the reproducibility for initiating SCC of OFP Cu (Ikeda and Litke 2004). As shown in

Table 4, the final copper concentrations in the solution after testing were higher than the initial copper concentrations as oxidation of the copper specimens continued during testing. The heavily etched appearance of the specimen surfaces (Figure 4) may be partly due to the long exposure period used for these experiments.

The results of experiments performed in ammonia solutions both with and without added copper were found to be similar. SCC was found in specimens tested in 1 mol·L⁻¹ ammonia solution with added copper (Table 2). The addition of 0.5 mol·L⁻¹ chloride did not suppress SCC (CERT109). However, the results of CERT108 indicated that a chloride concentration of ~5.5 mol·L⁻¹ would suppress SCC.

The potential transient obtained in the presence of added copper was similar to that observed in the absence of added copper. The potential was negative at the beginning of the experiment and then gradually shifted to more positive values. Ductile tearing and decreased load-bearing area was observed whilst the potential was < -0.40 V_{SCE}. A sharp transition from -0.40 to -0.30 V_{SCE} occurred for specimens susceptible to SCC. In contrast to the experiments performed without added copper, the positive-going transition was observed earlier (between 250 and 300 h) in the presence of added copper.

All specimens exhibited surface discolouration (Figure 4). No SCC was observed for the specimen exposed to the saturated chloride solution (CERT108). This specimen was tinted a bluish colour, the copper concentration after the experiment was high, and the corrosion potential remained negative throughout the experiment despite the high copper concentration. Exposing OFP Cu to 0.5 mol·L⁻¹ chloride (CERT109) produced a heavy oxidation coating (Figure 4), a final solution concentration of copper similar to that observed for the saturated chloride solution, and the lowest SCCF1 value (Table 4). The copper concentration was consistently lower in the absence of chloride (CERT70, CERT74, CERT76). However, the specimen surfaces had a moderate amount of surface oxidation and the values of the SCCF1 and SCER were in a range similar to the 0.5 mol·L⁻¹ chloride test (Table 4).

3.3 EFFECT OF HIGH CHLORIDE CONCENTRATION IN 0.1 mol·L⁻¹ ACETATE SOLUTION

The experimental conditions and results of tests performed galvanostatically, using 1 μA·cm⁻² applied current, in deaerated 0.1 mol·L⁻¹ acetate at pH 9, are shown in Tables 2 and 5.

In previous experiments, small SCC cracks were observed in copper specimens in chloride-free solution (CERT92) and in solutions containing 0.001 mol·L⁻¹ NaCl (CERT102). No significant crack propagation was observed in these specimens (Figure 5). With the addition of 0.01 and 0.1 mol·L⁻¹ NaCl, only ductile tearing and no SCC were observed (CERT101 and CERT100, Figure 5). In the present study, the addition of ~5.5 mol·L⁻¹ NaCl also resulted in pure ductile tearing and no SCC (CERT106).

In general, the specimen surfaces were discoloured with a purplish film and included the presence of a patchy brownish/blackish oxide (Figure 5, Table 2). The largest amount of dark, black oxide was observed on the specimen exposed to 0.001 mol·L⁻¹ chloride solution. The amount of the brown/black oxide decreased with increasing chloride concentration. The specimen exposed to saturated chloride solution did not show extensive film formation, but was heavily etched. The copper concentration in the saturated chloride solution was high, while in the solutions with added chloride concentrations of 0.1 mol·L⁻¹ or less the copper concentration

was negligible. As the addition of chloride concentration was increased, the uniform corrosion rate would increase and the amount of oxide film formation would also be reduced. No oxide film was found on the specimen of CERT106, which was carried out in saturated NaCl.

The load- and potential-transient plots are shown in Figure 5, with an overview image of the specimen following the completion of each acetate experiment shown to the left of each graph. The load curves for Cu specimens exposed to 0.1 mol·L⁻¹ acetate solutions containing 0.1 and 5.5 mol·L⁻¹ NaCl (CERT100 and CERT106) were fairly flat, indicating ductile tearing of these specimens (Figure 5). The shape of the load curves for Cu specimens exposed to 0.1 mol·L⁻¹ acetate solutions containing 0, 0.001, and 0.1 mol·L⁻¹ NaCl (CERT92, CERT102, and CERT101) suggests some degree of brittle-like cracking (Figure 5). These curves did not decay with the rapidity characteristic of SCC in nitrite or ammonia solutions, but underwent a continual, moderate decline. The potential of the specimen usually shifted positive over the initial 100 h of the experiment, then reached a steady state value that decreased from 0.1 V_{SCE} in the absence of chloride, to -0.38 V_{SCE} in saturated chloride. The steady state potential shifted to more negative values with increasing chloride concentration. A large negative shift occurred between 0.1 mol·L⁻¹ and saturated chloride concentrations.

For CERT100 and CERT106, the large SCCF1 values (i.e., >5) and small SCER (i.e., less than 2 nm·s⁻¹) were consistent with the absence of SCC observed in these specimens (Table 5). The lower values for SCCF1 measured in the remaining experiments in this series (0.1 mol·L⁻¹ acetate containing ≤ 0.01 mol·L⁻¹ NaCl) suggest mixed mode cracking. The results of the tests in 0.1 mol·L⁻¹ acetate suggest that the critical potential for cracking lies somewhere between 0.05 and 0.15 V_{SCE} (Figure 5).

4. CONCLUSIONS

Based on the SCC tests performed in this study and an assessment of previous SCC test results, the effect of NaCl concentrations can be summarized as follows:

- In a 0.1 mol·L⁻¹ nitrite solution, copper could be subjected to extensive SCC in the presence of ≤ 0.01 mol·L⁻¹ (i.e., ~0.6 g·L⁻¹) NaCl. However, the addition of 0.1 mol·L⁻¹ (~6 g·L⁻¹) and 5.5 mol·L⁻¹ (i.e., ~320 g·L⁻¹) NaCl would suppress SCC.
- In a 1 mol·L⁻¹ ammonia solution, copper could be subjected to extensive SCC in the absence of NaCl and in the presence of 0.5 mol·L⁻¹ (~30 g·L⁻¹) NaCl. However, the addition of ~5.5 mol·L⁻¹ (~320 g·L⁻¹) NaCl would suppress SCC.
- In a 0.1 mol·L⁻¹ acetate solution, copper could be susceptible to SCC in the presence of ≤ 0.01 mol·L⁻¹ NaCl. However, the extent of SCC would be limited. An addition of 0.1 or ~5.5 mol·L⁻¹ (i.e., 6 g·L⁻¹ and 320 g·L⁻¹) NaCl suppressed SCC and the copper specimens were only subjected to ductile tearing.

The present study appears to indicate a high concentration of NaCl (~5.5 mol·L⁻¹, ~320 g·L⁻¹) would suppress SCC in nitrite, ammonia, and acetate solutions. The high NaCl concentration would suppress SCC by promoting uniform corrosion and disrupting oxide film formation on the crack surface. The stress corrosion factor (SCCF1), surface crack extension rate (SCER), and visual examination of the copper specimens suggested ductile behaviour in high chloride concentrations.

ACKNOWLEDGEMENTS

The authors wish to acknowledge the support and assistance of P. Maak throughout this project. We also wish to acknowledge R. Herman for performing the chemical analysis, K.D. Jackson for instrumentation support, D.P. Godin for fatiguing the CT specimens, and J.P.L. David for the preparation of samples.

REFERENCES

- ASTM. 1994. Standard test method for plane-strain fracture toughness of metallic materials, 1994 Annual Book of ASTM Standards, Section 3, Volume 03.01. American Society for Testing and Materials, Philadelphia, PA, E 399-90.
- Bertocci, U., E.N. Pugh, and R.E. Ricker. 1990. "Environment-induced cracking of copper alloys". In *Environment-Induced Cracking of Metals*, NACE-10, (Editors R.P. Gangloff and M.B. Ives). National Association of Corrosion Engineers, Houston Tx. pp. 273-285.
- Cassagne, T.B., J. Kruger, and E.N. Pugh. 1990. Role of the oxide film in the transgranular stress corrosion cracking of copper. In *Environmentally Assisted Cracking: Science and Engineering*, ASTM STP 1049. (Editors, W.B. Lisagor, T.W. Crooker, and B.N. Leis), American Society for Testing and Materials, Philadelphia, PA. pp. 59-75.
- Honda, T., M. Yamashita, M. Kamio, H. Uchida, and H. Shirai. 1999. Stress Corrosion Cracking of Pure Copper in Acetic Acid Solutions. In *14th International Corrosion Congress*, Cape Town, South Africa, September 26-October 1, 1999, pp. 19-67
- Ikeda, B.M. and C.D. Litke. 2000. The effect of oxidant flux, nitrite concentration and chloride concentration on the stress corrosion cracking behaviour of non-welded and electron-beam welded copper. Prepared by Atomic Energy of Canada Limited for Ontario Power Generation. Ontario Power Generation, Nuclear Waste Management Division Report 06819-REP-01200-10049-R00. Toronto, Ontario.
- Ikeda, B.M. and C.D. Litke. 2004. Status report for 2003 on stress corrosion cracking of OFP copper in ammonia. Ontario Power Generation, Nuclear Waste Management Division Report 06819-REP-01300-10078-R00. Toronto, Ontario.
- King, F. and M. Kolar. 2005. Preliminary assessment of the stress corrosion cracking of used fuel disposal containers using the CCM-SCC.0 model. Ontario Power Generation, Nuclear Waste Management Division Report 06819-REP-01300-10103-R00. Toronto, Ontario.
- King, F., C.D. Litke and B.M. Ikeda. 1999a. The effects of oxidant supply and chloride ions on the stress corrosion cracking of copper. Ontario Power Generation, Nuclear Waste Management Division Report 06819-REP-01200-10013-R00. Toronto, Ontario.
- King, F., G. Greidanus and D.J. Jobe. 1999b. Dissolution of copper in chloride/ammonia mixtures and the implications for the stress corrosion cracking of copper containers. Atomic Energy of Canada Limited Report, AECL-11865, COG-97-412-I.
- King, F., L. Ahonen, C. Taxén, U. Vuorinen, and L. Werme. 2001. Copper corrosion under expected conditions in a deep geologic repository. Swedish Nuclear Fuel and Waste Management Co. Report TR-01-23.
- King, F., L. Ahonen, C. Taxén, U. Vuorinen, and L. Werme. 2002. Copper corrosion under expected conditions in a deep geologic repository. Posiva Report POSIVA 2002-01.

Litke, C.D., and B.M. Ikeda. 2006. The effect of acetate concentration, chloride concentration, and applied current on stress corrosion cracking of OFP copper. Ontario Power Generation, Nuclear Waste Management Division Report 06819-REP-01300-10005-R00. Toronto, Ontario.

Maak, P. 1999. The selection of a corrosion-barrier primary material for used-fuel disposal containers. Ontario Power Generation, Nuclear Waste Management Division Report 06819-REP-01200-10020 R00. Toronto, Ontario.

Table 1: Summary of Chloride Experiments Performed* at Room Temperature

Test Number	[Solution] mol·L ⁻¹	[CuSO ₄] Added mmol·L ⁻¹	[NaCl] Added mol·L ⁻¹	pH Initial	pH Final	Conditions	[Cu] [†] (in Solution) mmol·L ⁻¹	E _{corr} Final V	E _{red} Final V	Total Time h	K _Q MPa·m ^½	SCCF1	Crack Velocity mm·a ⁻¹	Crack Velocity nm·s ⁻¹
CERT106	0.1 (Acetate)	0	Sat'd	9	9.1	1 μA/cm ²	0.13	-0.363	-0.012	410.5	21.7	6.09	59	1.9
CERT107	0.1 (Nitrite)	0	Sat'd	9	9.8	1 μA/cm ²	0.27	-0.374	0.011	428.2	20.0	6.54	56	1.8
CERT108	1.0 (Ammonia)	4	Sat'd	11.6	12.5	1 μA/cm ²	42.5	-0.462	-0.277	502.7	22.0	6.04	63	2.0
CERT109	1.0 (Ammonia)	4	0.5	12.1	12.8	1 μA/cm ²	45.6	-0.285	0.043	432.0	21.2	2.39	169	5.3
CERT110	1.0 (Ammonia)	0	0.5	12.0	12.7	1 μA/cm ²	39.3	-0.293	-0.228	526.0	20.6	3.00	129	4.1
CERT111	1.0 (Ammonia)	0	Sat'd	11.9	12.4	1 μA/cm ²	17.3	-0.473	-0.259	595.8	20.9	5.70	67	2.1

* All experiments performed in deaerated solution at 22 ± 2°C, at a cross-head speed of 8.5 x 10⁻⁶ mm·s⁻¹ with SKB4 compact tension specimens cut from plate, Sections C1D and C1E (CERT111) in a TS orientation

† 2σ error interval ± 10% for CERT106, CERT107, CERT109 and CERT111; ± 11% for CERT108; and ± 8% for CERT110

Table 2: Summary of Comparative Experimental Results in All Environments

Test number	Base solution	Chloride mol/L	Other	pH	Current μA	SCER ($\text{nm}\cdot\text{s}^{-1}$)	SCC Factor 1	SCC	Observed Crack	Observed Surface
CERT107	0.1M Nitrite	Sat	deaerated	9	1	1.77	6.54	no	ductile	Coarsely etched surface with purple/light brown/red/blue mottled oxidation
CERT35	0.1M Nitrite	0.1	deaerated	9	1	2.08	5.62	no	blunt ductile	Uniform loosely adherent heavy purple film which flaked off in the ductile zone. Surface bright under film.
CERT29	0.1M Nitrite	0.01	deaerated	9	1	4.40	2.70	yes	multiple SCC cracks	Oxidized brown/blue/purple surface, heavier on exposed portions, darker in ductile zone
CERT30	0.1M Nitrite	0.001	deaerated	9	1	7.66	1.37	yes	several small SCC cracks (very short duration exp't)	Mottled brown/blue/purple/pink surface. Heavier on exposed portions.
CERT43	0.1M Nitrite	0	deaerated	9	1	8.86	1.34	yes	large SCC crack, multiple small and medium SCC cracks	Heavier blue/brown ppte over most of surface. Some bright/pink areas.
CERT27	0.1M Nitrite	0	deaerated	9	1	7.27	1.66	yes	large SCC crack, multiple small and medium SCC cracks	Mottled bright/blue/pink surface. Heavier blue/brown ppte in ductile zone.
CERT111	1M NH ₃	Sat	aerated	12	1	2.12	5.70	no	blunt ductile	Etched surface covered with uniform brown/purple oxidation. Some bright spots and black ppte
CERT110	1M NH ₃	0.5	aerated	12	1	4.07	3.00	yes	large SCC cracks, multiple small SCC cracks	Oxidized brown/purple/blue surface, heavier on exposed portions. Severe dissolution attack. Some bright areas and black ppte present.
CERT66	1M NH ₃	0	aerated	12	1	3.38	3.66	yes	multiple SCC cracks	Oxidized brown surface discolouration, darker purple/brown on etched portion
CERT67	1M NH ₃	0	aerated	12	1	3.28	3.84	yes	multiple SCC cracks	Oxidized brown surface discolouration, darker on etched portion
CERT68	1M NH ₃	0	aerated	12	1	2.46	4.92	no	ductile, indication of couple secondary cracks on fracture surface	Bright, shiny grey etched surface
CERT108	1M NH ₃	Sat	air/4mM Cu	12	1	1.98	6.04	no	blunt ductile	Finely etched surface with a mixture of bright spots and uniform brown/some purple oxidation
CERT109	1M NH ₃	0.5	air/4mM Cu	12	1	5.34	2.39	yes	large SCC crack, multiple small SCC cracks	Oxidized black/brown/blue surface on exposed portions. Severe dissolution attack. Some bright areas and brown red oxidation on area under grips.
CERT70	1M NH ₃	0	air/4mM Cu	12	1	3.88	3.24	yes	multiple large SCC cracks	Oxidized brown surface discolouration, darker purple/brown on etched portion
CERT74	1M NH ₃	0	air/4mM Cu	12	1	4.81	2.54	yes	multiple large SCC cracks	Oxidized brown surface discolouration, darker purple/brown on etched portion
CERT76	1M NH ₃	0	air/4mM Cu	12	1	3.44	2.55	yes	multiple large SCC cracks	Oxidized brown/green surface discolouration, patches of green oxide, pits, purple/blue-green film on crack faces
CERT106	0.1M Acetate	Sat	deaerated	9	1	1.87	6.09	no	ductile	Coarsely etched surface with varying shades of brown and some purple/red/blue mottled oxidation
CERT100	0.1M Acetate	0.1	deaerated	9	1	1.73	6.82	no	blunt ductile	Oxidized purple/brown surface, uniform
CERT101	0.1M Acetate	0.01	deaerated	9	1	2.55	4.73	no	ductile, secondary cracks on fracture surface	Oxidized brown/purple/blue surface, heavier on exposed portions
CERT102	0.1M Acetate	0.001	deaerated	9	1	3.70	3.22	yes	1 small SCC cracks	Oxidized purple/brown surface, some lighter blotches, less uniform, heavy black oxide on exposed surfaces
CERT92	0.1M Acetate	0	deaerated	9	1	2.93	4.00		ductile, multiple small SCC cracks	Bright, some portions of exposed surface covered in blue-grey film, purple oxidation around crack mouth

Table 3: Summary of Experiments as a Function of Chloride Concentration in 0.1 mol-L⁻¹ Nitrite Solutions

Test Number	[Chloride] mol-L ⁻¹	pH Initial	Conditions	[Cu] [†] (in Solution) mmol-L ⁻¹	E _{corr} Final V	E _{red} Final V	Total Time h	K _q MPa·m ^½	SCCF1	SCER mm·a ⁻¹	SCER nm·s ⁻¹
CERT107	Sat'd	9	1 μA/cm ²	0.271	-0.374	0.011	428.2	20.0	6.54	55.7	1.77
CERT35	0.1	9	1 μA/cm ²	0.008	-0.135	-	331.9	21.0	5.62	65.6	2.08
CERT29	0.01	9	1 μA/cm ²	0.013	0.070	-	333.2	26.3	2.70	139	4.40
CERT30	0.001	9	1 μA/cm ²	0.009	-	-	51.1	21.5	1.37	241	7.66
CERT43	0	9	1 μA/cm ²	0.002	0.122	-	168.0	16.2	1.34	280	8.86
CERT27	0	9	1 μA/cm ²	0.009	0.040	-	257.7	23.4	1.66	229	7.27

† 2σ error interval ± 10%

Table 4: Summary of Experiments as a Function of Chloride Concentration in 1 mol-L⁻¹ Ammonia Solutions

Test Number	[Chloride] mol-L ⁻¹	[Cu] Added mmol-L ⁻¹	pH Initial	pH Final	Conditions	[Cu] [†] (in Solution) mmol-L ⁻¹	[Cl] (in Solution) mmol-L ⁻¹	E _{corr} Final V	E _{red} Final V	Total Time h	K _q MPa·m ^½	SCCF1	SCER mm·a ⁻¹	SCER nm·s ⁻¹
CERT111	Sat	0	11.9	12.4	1 μA/cm ²	17.3	-	-0.473	-0.259	595.8	20.9	5.70	66.7	2.12
CERT110	0.5	0	12.0	12.7	1 μA/cm ²	39.3	-	-0.293	-0.228	526.0	20.6	3.00	129	4.07
CERT66	0	0	11.7	-	1 μA/cm ²	19.7	2.17	-0.277	-	624.5	18.5	3.66	107	3.38
CERT67	0	0	11.7	-	1 μA/cm ²	17.5	1.21	-	-	624.0	23.5	3.84	104	3.28
CERT68	0	0	11.7	-	1 μA/cm ²	17.3	3.67	-0.403	-	524.6	20.6	4.92	77.7	2.46
CERT108	Sat	4	11.6	12.5	1 μA/cm ²	42.5	-	-0.462	-0.277	502.7	22.0	6.04	62.6	1.98
CERT109	0.5	4	12.1	12.8	1 μA/cm ²	45.6	-	-0.285	0.043	432.0	21.2	2.39	169	5.34
CERT70	0	4	11.6	-	1 μA/cm ²	27.1	12.4	-0.267	-	501.4	23.7	3.24	123	3.88
CERT74	0	4	11.7	-	1 μA/cm ²	26.8	3.44	-0.268	-	476.6	23.3	2.54	152	4.81
CERT76	0	4	11.7	-	1 μA/cm ²	31.5	0.99	-0.265	-	575.4	24.2	2.55	109	3.44

† 2σ error interval ± 10%

Table 5: Summary of Experiments as a Function of Chloride Concentration in 0.1 mol-L⁻¹ Acetate Solutions

Test Number	[Chloride] mol-L ⁻¹	pH Initial	Conditions	[Cu] [†] (in Solution) mmol-L ⁻¹	E _{corr} Final V	E _{red} Final V	Total Time h	K _Q MPa·m ^{1/2}	SCCF1	SCER mm·a ⁻¹	SCER nm·s ⁻¹
CERT106	Sat'd	9	1 μA/cm ²	0.127	-0.363	-0.012	410.5	21.7	6.09	58.8	1.87
CERT100	0.1	9	1 μA/cm ²	0.002	-0.101	0.073	360.4	22.6	6.82	54.5	1.73
CERT101	0.01	9	1 μA/cm ²	0.002	0.031	0.083	360.7	23.9	4.73	80.3	2.55
CERT102	0.001	9	1 μA/cm ²	0.002	0.050	0.094	334.6	20.6	3.22	117	3.70
CERT92	0	9	1 μA/cm ²	0.094	0.117		306.6	24.6	4.00	92.4	2.93

[†] 2σ error interval ± 10%

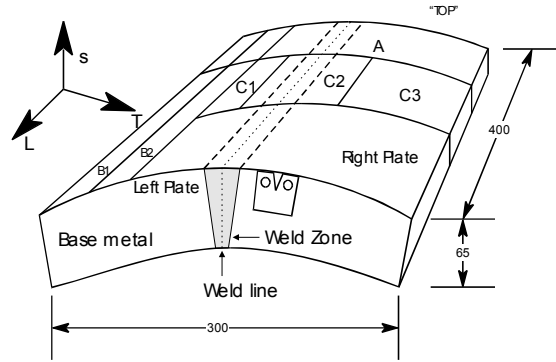


Figure 1: Schematic of SKB4 Plate Material Showing the Location of Specimen Cuts.

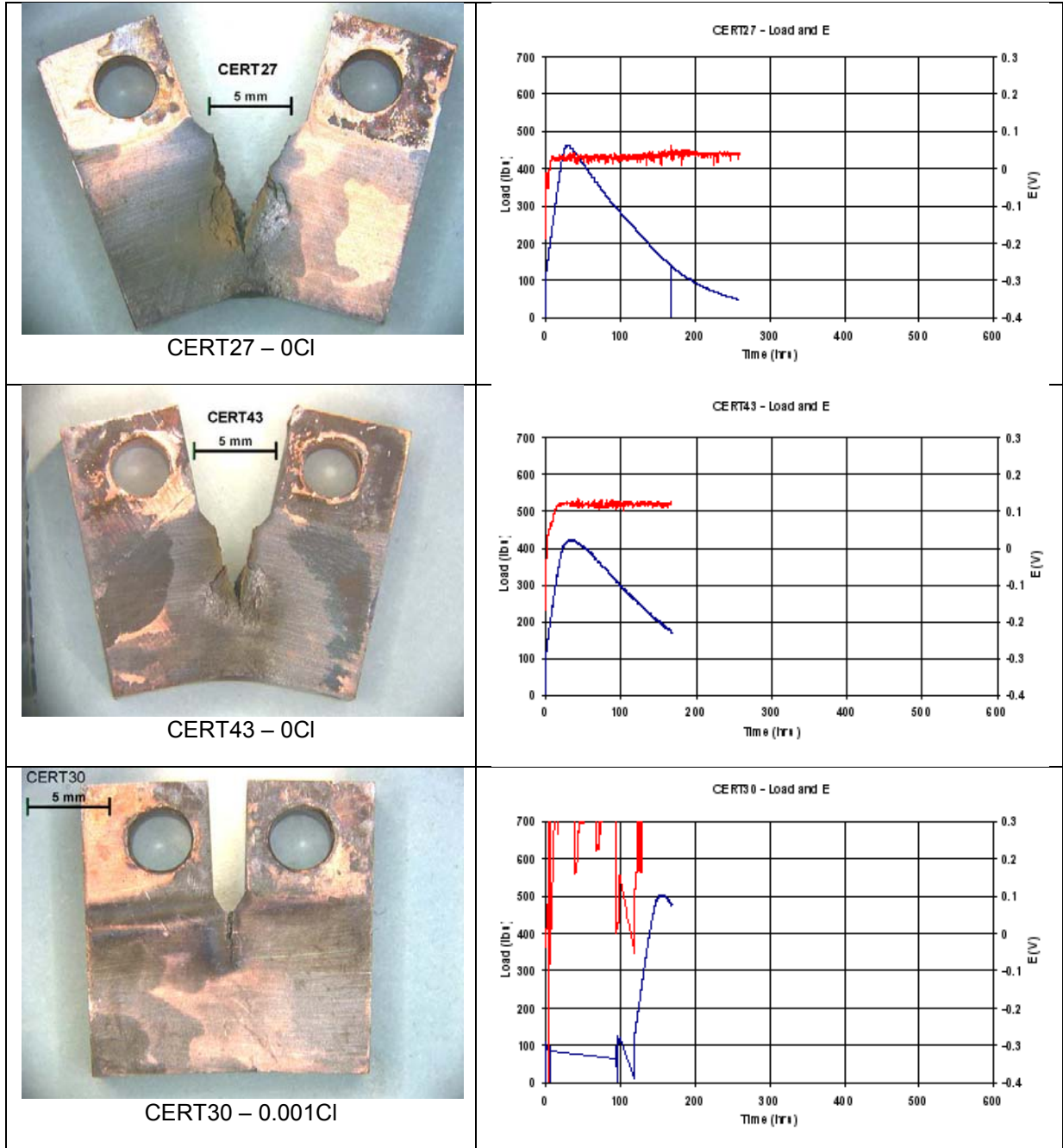


Figure 2: Compilation of SCC behaviour for OFP Cu in Chloride-containing deaerated 0.1 mol·L⁻¹ Nitrite solution.

A plot of the potential (red line) and load (blue line) behaviour as a function of time is shown to the right of an overview image of the specimen. The test number and the chloride concentration for the test are given below each image.

Figure 2 continues ...

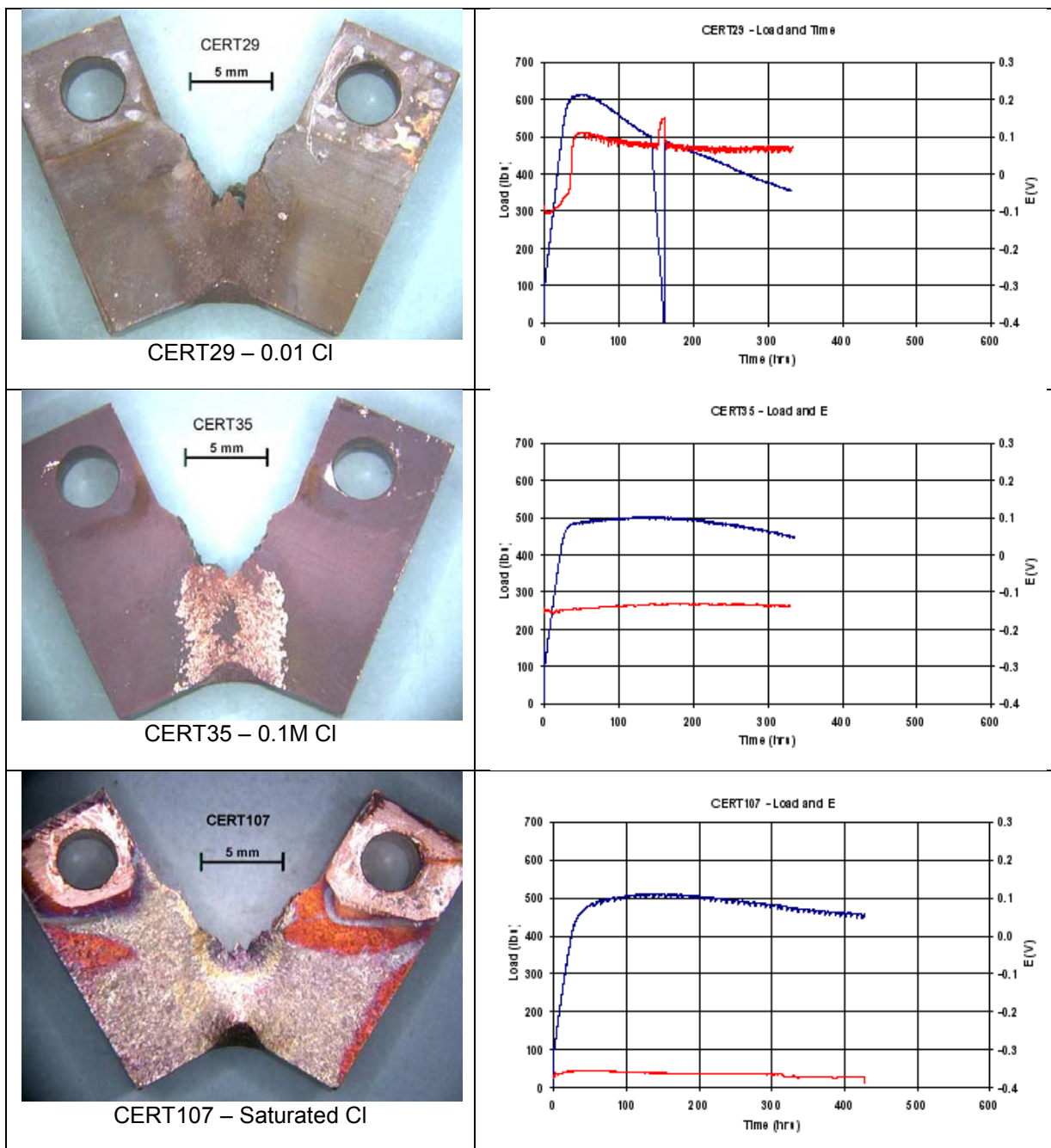


Figure 2 Concluded: Compilation of SCC behaviour for OFF Cu in Chloride-containing deaerated 0.1 mol-L⁻¹ Nitrite solution.

A plot of the potential (red line) and load (blue line) behaviour as a function of time is shown to the right of an overview image of the specimen. The test number and the chloride concentration for the test are given below each image.

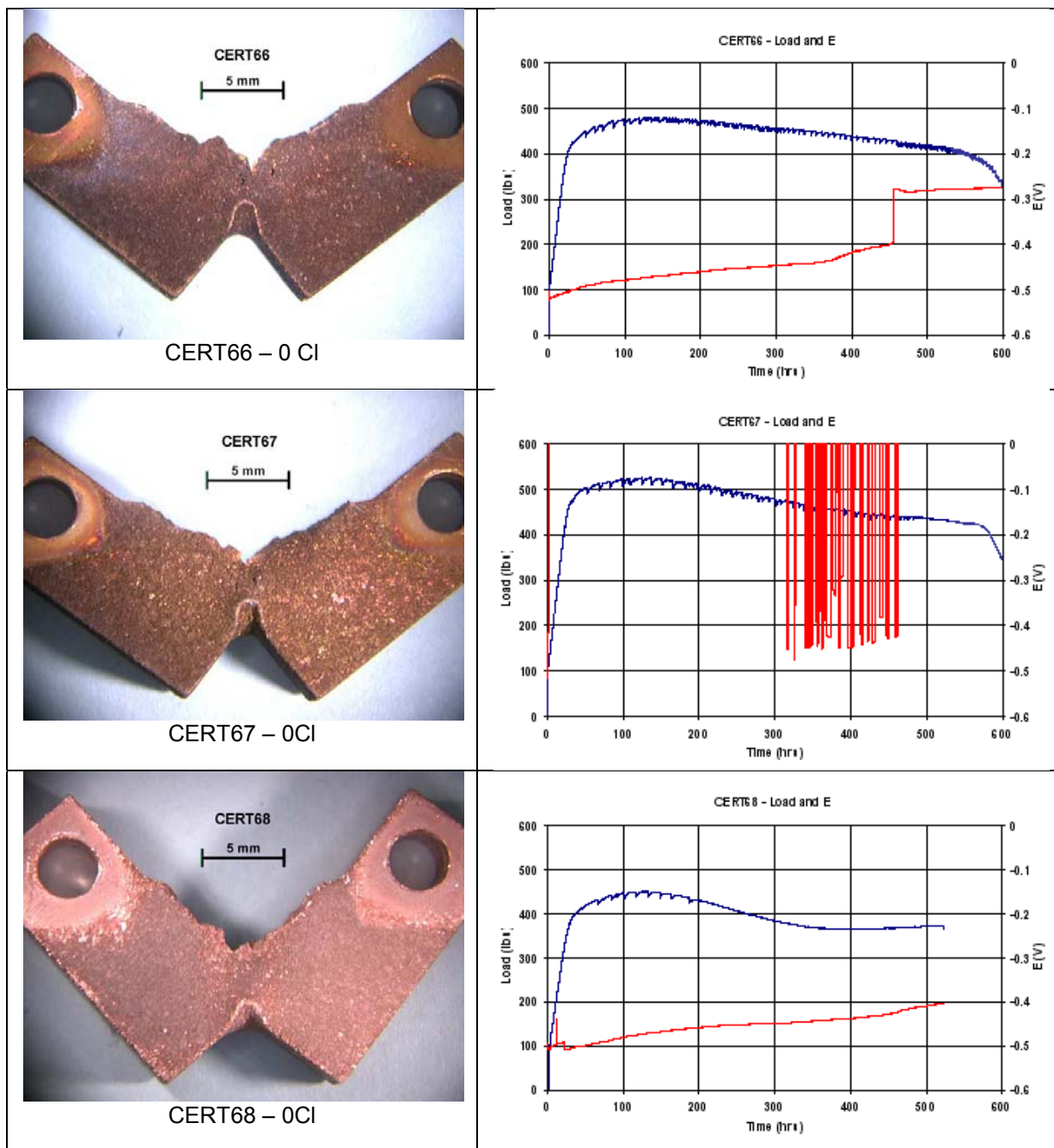


Figure 3: Compilation of SCC behaviour for OFP Cu in Chloride-containing aerated 1 mol-L⁻¹ Ammonia solution without added copper.
A plot of the potential (red line) and load (blue line) behaviour as a function of time is shown to the right of an overview image of the specimen. The test number and the chloride concentration for the test are given below each image.

Figure 3 continues ...

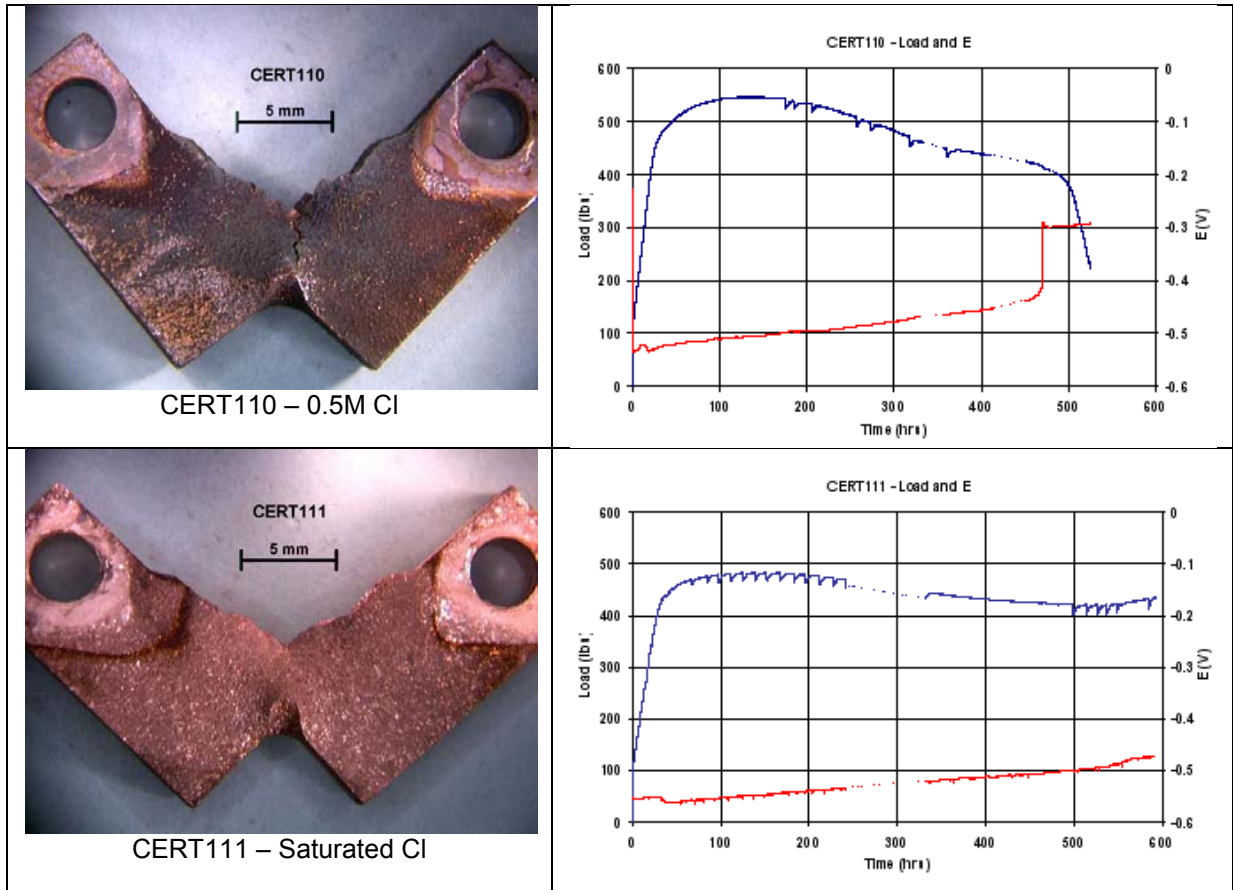


Figure 3 Concluded: Compilation of SCC behaviour for OFF Cu in Chloride-containing aerated 1 mol·L⁻¹ Ammonia solution without added copper.

A plot of the potential (red line) and load (blue line) behaviour as a function of time is shown to the right of an overview image of the specimen. The test number and the chloride concentration for the test are given below each image.

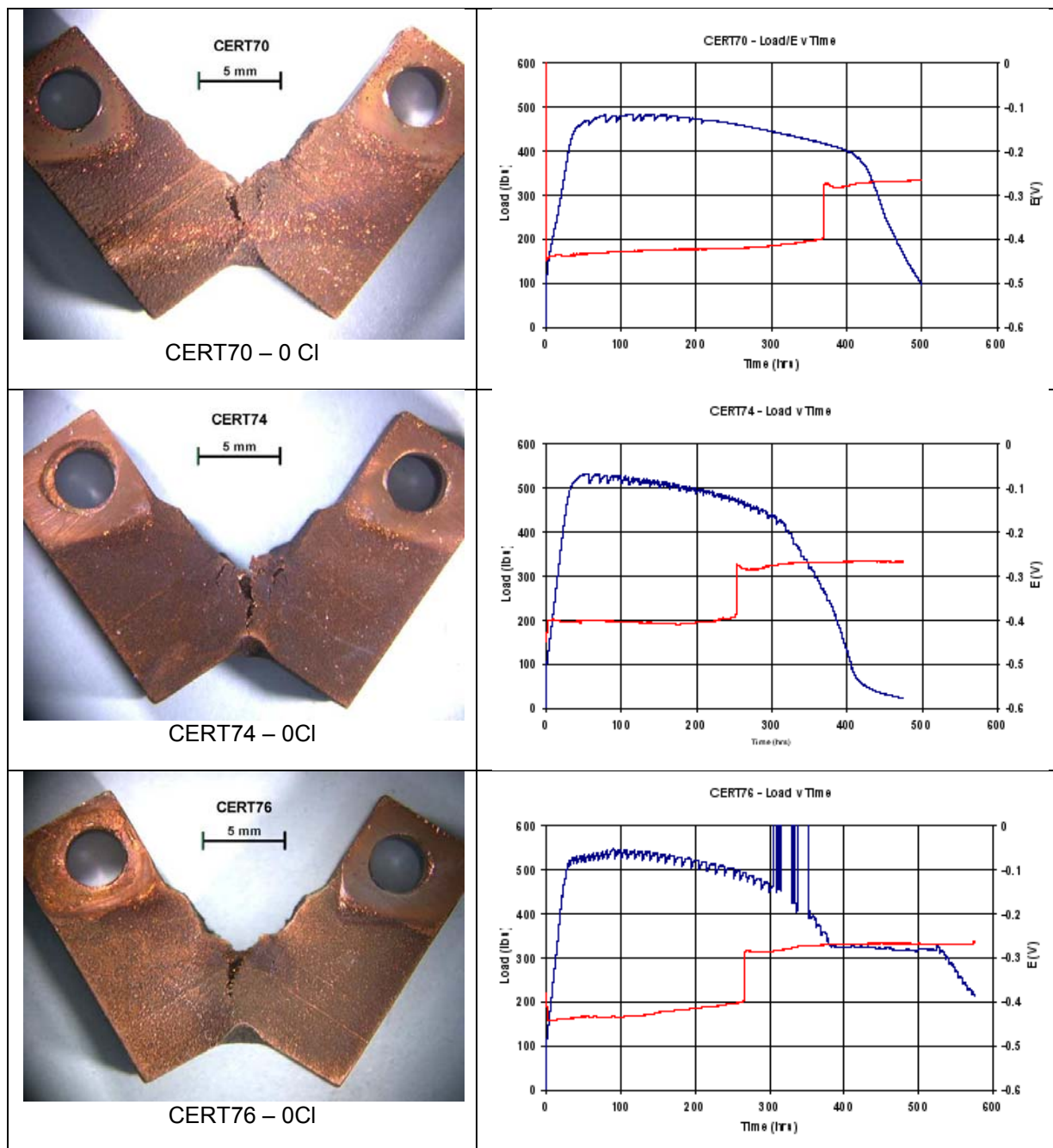


Figure 4: Compilation of SCC behaviour for OFF Cu in Chloride-containing aerated 1 mol·L⁻¹ Ammonia solution with 4 mmol·L⁻¹ added copper.

A plot of the potential (red line) and load (blue line) behaviour as a function of time is shown to the right of an overview image of the specimen. The test number and the chloride concentration for the test are given below each image.

Figure 4 continues ...

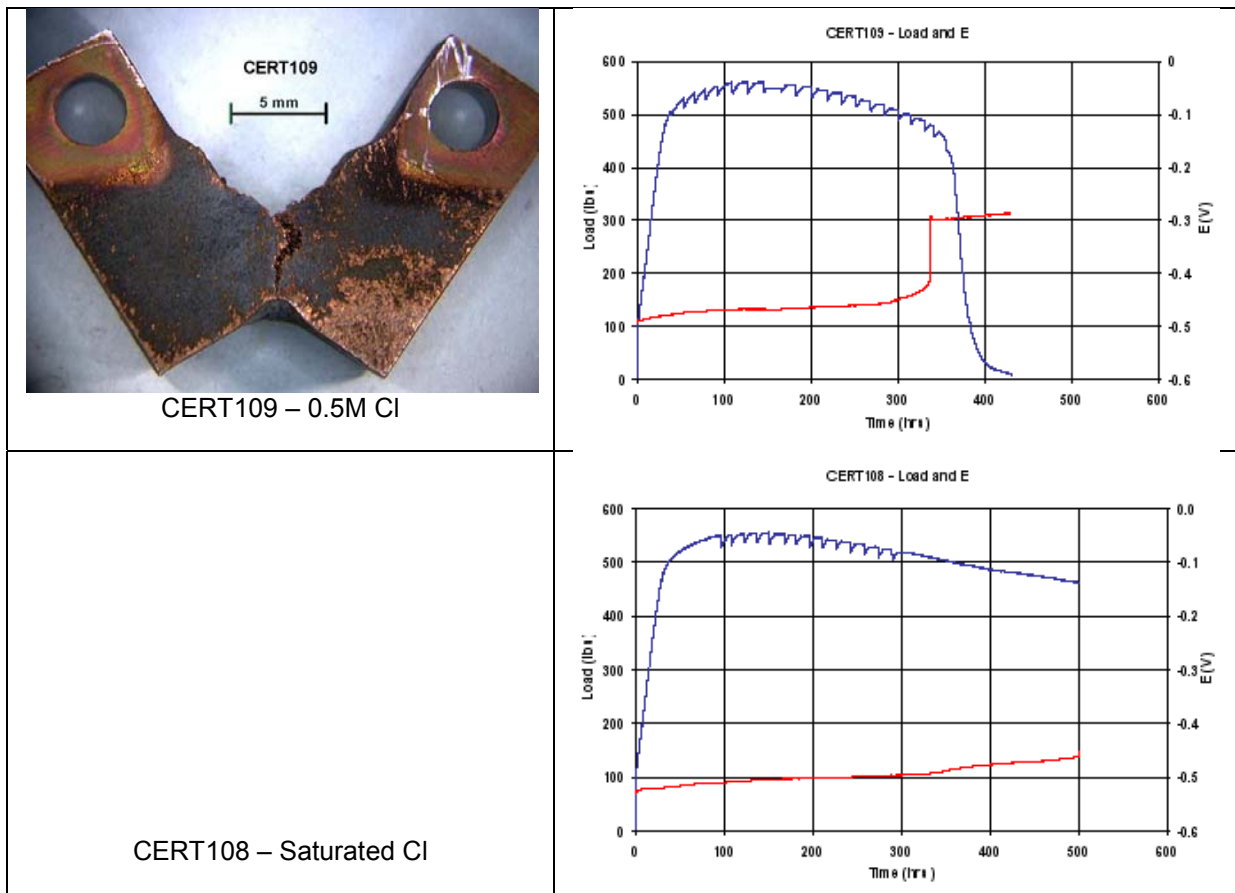


Figure 4 Concluded: Compilation of SCC behaviour for OFF Cu in Chloride-containing aerated 1 mol-L⁻¹ Ammonia solution with 4 mmol-L⁻¹ added copper. A plot of the potential (red line) and load (blue line) behaviour as a function of time is shown to the right of an overview image of the specimen. The test number and the chloride concentration for the test are given below each image.

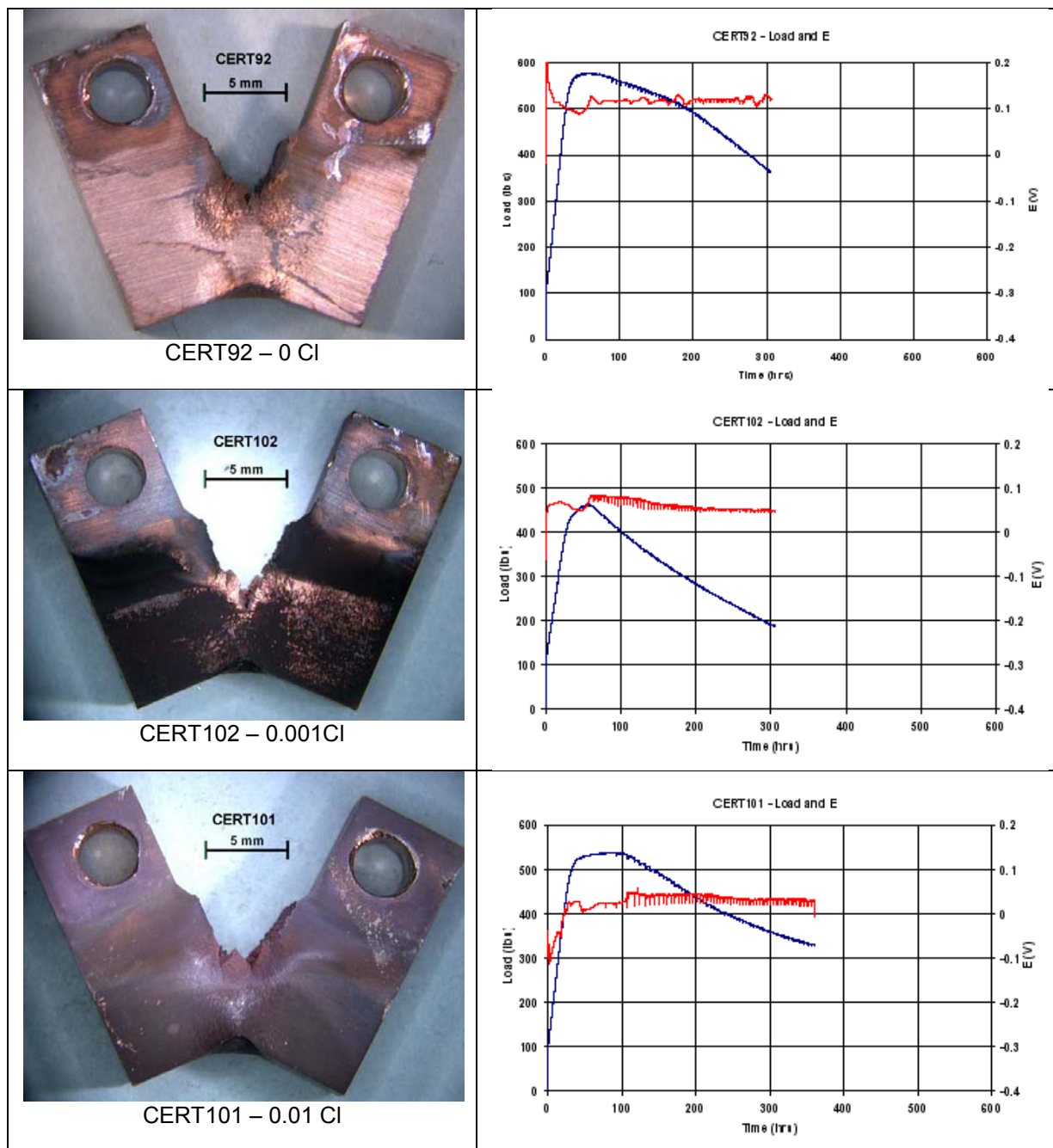


Figure 5: Compilation of SCC behaviour for OFP Cu in Chloride-containing deaerated 0.1 mol-L⁻¹ Acetate solution.

A plot of the potential (red line) and load (blue line) behaviour as a function of time is shown to the right of an overview image of the specimen. The test number and the chloride concentration for the test are given below each image.

Figure 5 Continues ...

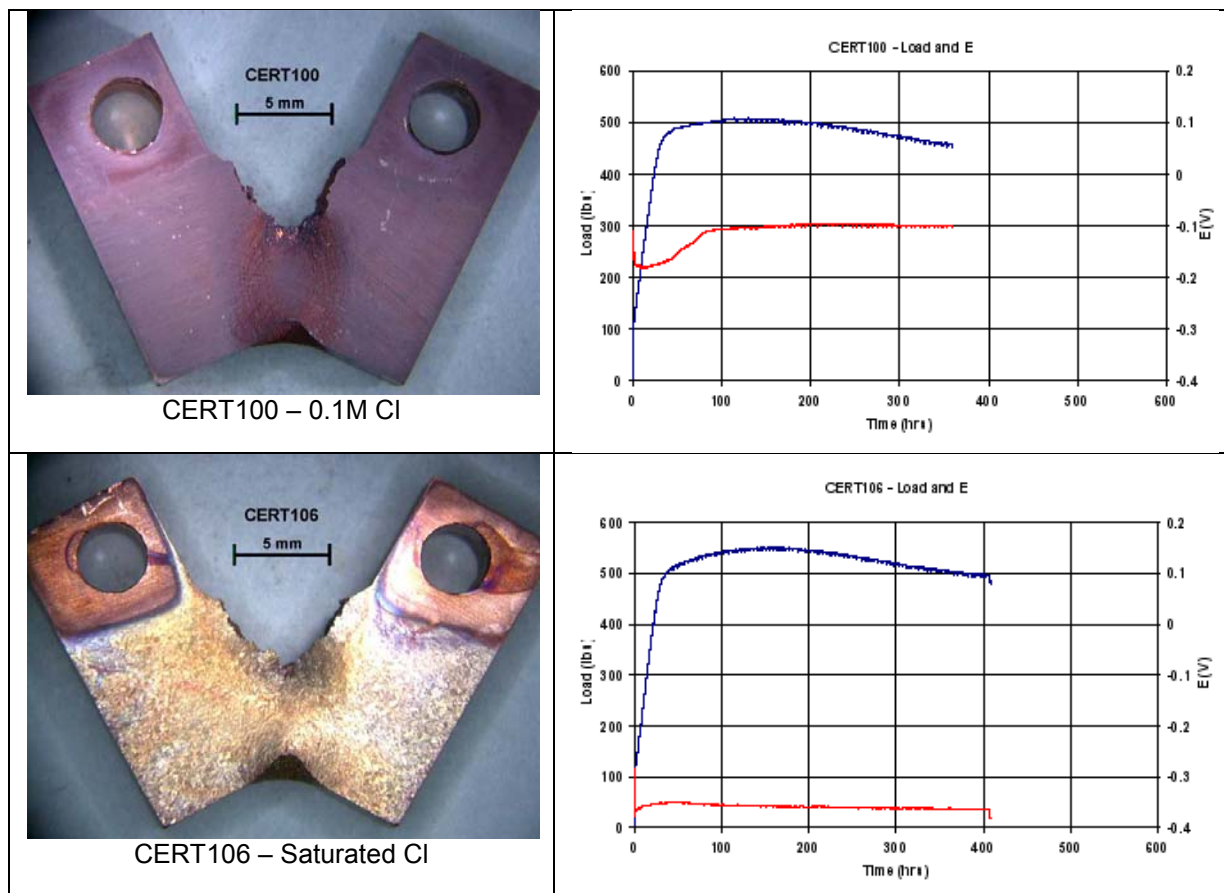


Figure 5 Concluded: Compilation of SCC behaviour for OFFP Cu in Chloride-containing deaerated 0.1 mol·L⁻¹ Acetate solution.

A plot of the potential (red line) and load (blue line) behaviour as a function of time is shown to the right of an overview image of the specimen. The test number and the chloride concentration for the test are given below each image.